

# Erodibility of cohesive streambeds in the loess area of the midwestern USA

G. J. Hanson<sup>1\*</sup> and A. Simon<sup>2</sup>

<sup>1</sup> USDA—Agricultural Research Service, Stillwater, OK, USA

<sup>2</sup> USDA—Agricultural Research Service, Oxford, MS, USA

---

## Abstract:

Excess stress parameters, critical shear stress ( $\tau_c$ ) and erodibility coefficient ( $k_d$ ), for degrading channels in the loess areas of the midwestern USA are presented based on *in situ* jet-testing measurements. Critical shear stress and  $k_d$  are used to define the erosion resistance of the streambed. The jet-testing apparatus applies hydraulic stresses to the bed and the resulting scour due to the impinging jet is related to the excess stress parameters. Streams tested were primarily silt-bedded in texture with low densities, which is typical of loess soils. Results indicate that there is a wide variation in the erosion resistance of streambeds, spanning six orders of magnitude for  $\tau_c$  and four orders of magnitude for  $k_d$ . Erosion resistance was observed to vary within a streambed, from streambed to streambed, and from region to region. An example of the diversity of materials within a river system is the Yalobusha River Basin in Mississippi. The median value of  $\tau_c$  for the two primary bed materials, Naheola and Porters Creek Clay Formations, was 1.31 and 256 Pa, respectively. Streambeds composed of the Naheola Formation are readily eroded over the entire range of shear stresses, whereas only the deepest flows generate boundary stresses great enough to erode streambeds composed of the Porters Creek Clay Formation. Therefore, assessing material resistance and location is essential in classifying and modelling streambed erosion processes of these streams.

KEY WORDS cohesive materials; erodibility; critical shear stress; jet-test device; midwestern USA

## INTRODUCTION

Areas of deep loess deposits in the midwestern USA (Figure 1) have experienced considerable land loss, entrenched streams and damage to infrastructure as a result of stream channel degradation. Stream channel degradation increases bank height, which destabilizes channel banks. The amount of bed degradation is a function of the type of bed material and its resistance to erosion, and the flow characteristics. An assessment of the resistance and distribution of channel materials is essential for classification and modelling the erosion processes of these streams.

Assessing erosion resistance of cohesive materials by flowing water is complex. The many studies that have been conducted on erodibility of cohesive materials have observed that numerous soil properties influence erosion resistance, including antecedent moisture, clay mineralogy and proportion, density, soil structure, organic content, as well as pore and water chemistry (Grissinger, 1982). These observations were made using a variety of experimental procedures. Test equipment has included straight and circular flumes, pipes, pinhole-testing apparatus, submerged jets, water tunnels, rotating cylinders, disks and propellers (Grissinger, 1982). This paper summarizes the use of an *in situ* submerged jet-testing apparatus to measure the erosion resistance of several streambeds in the loess areas of the midwestern USA (Figure 1). This device has been developed based on knowledge of the hydraulic characteristics of a submerged jet and the erodibility characteristics of soil-material ( $k_d$ ). The test is simple, quick and relatively inexpensive to perform. The test is repeatable and

---

\*Correspondence to: Gregory J. Hanson, USDA—Agricultural Research Service, 1301 N. Western St., Stillwater, OK 74075-2714, USA.

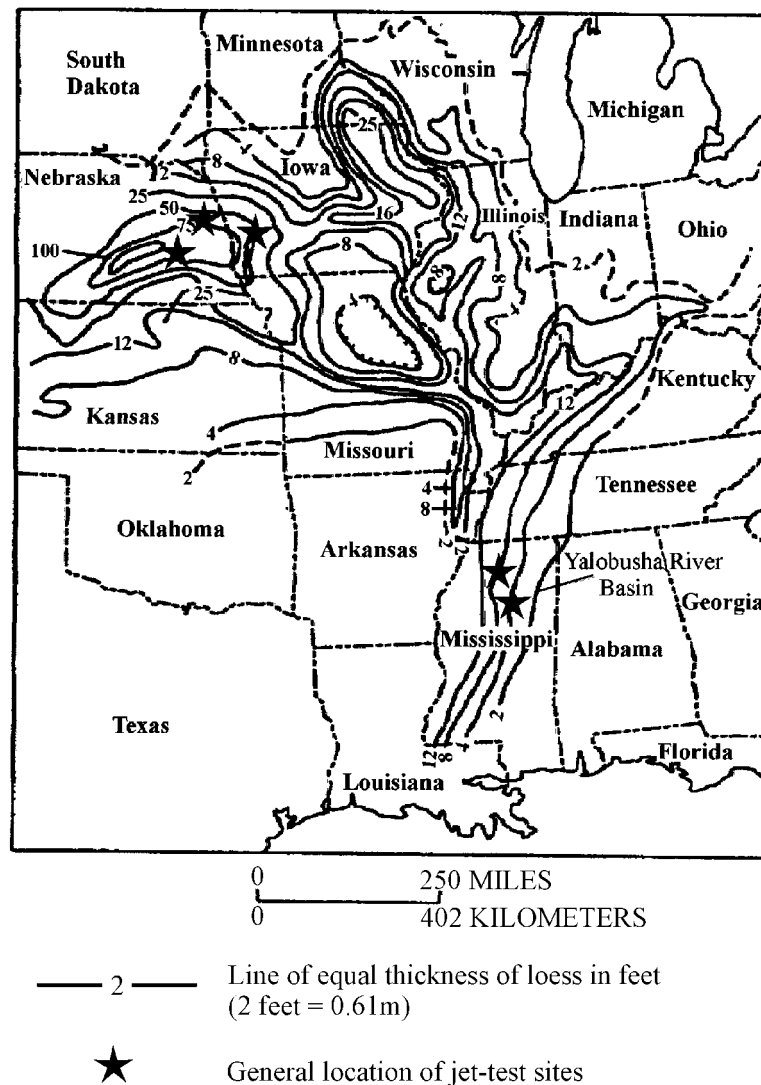


Figure 1. Map of loess area of the midwestern USA showing thickness of loess deposits and jet testing locations. Modified from Lutenecker (1987). Reprinted from Lutenecker AJ, *In situ* shear strength of friable loess. In *Loess and Environment*, copyright 1987, pages 27–34, with permission from Elsevier Science

gives consistent results. The coefficients obtained from test results can be used in current equations to predict erosion of cohesive materials.

It is assumed that the rate of erosion  $\varepsilon$  (in m/s) is proportional to the shear stress in excess of a critical shear stress expressed as

$$\varepsilon = k_d(\tau_e - \tau_c) \quad (1)$$

where  $k_d$  is the erodibility coefficient ( $\text{m}^3/\text{N-s}$ ),  $\tau_c$  is the critical shear stress (Pa) and  $\tau_e$  is the effective shear stress (Pa). This equation indicates that the effective shear stress must be greater than the critical shear stress to initiate erosion.

The jet apparatus is capable of applying a wide range of hydraulic shear stresses. Analytical procedures have been developed for determining the  $\tau_c$  and  $k_d$  from submerged jet-scour results (Hanson and Cook, 1997).

## BACKGROUND

A submerged jet test has been developed for testing of materials in the laboratory and in the field (ASTM, 1995). A number of studies have used a submerged jet for testing of materials in the laboratory (Dunn, 1959; Moore and Masch, 1962; Hollick, 1976; Hanson and Robinson, 1993). Recently a submerged jet test has been developed for testing materials *in situ* (Hanson, 1990). The work conducted by Dunn (1959), Moore and Masch (1962) and Hollick (1976) was for the purpose of determining critical shear stress. Hanson (1991) developed a soil-dependent jet index based on the change in maximum scour depth caused by an impinging jet. This development included an empirical relationship between the jet index and erosion.

In an attempt to remove empiricism and to obtain direct measurements of the excess stress parameters,  $\tau_c$  and  $k_d$ , Hanson and Cook (1997) developed analytical procedures for determining soil  $k_d$  based on the diffusion principles of a submerged circular jet and the corresponding scour. These procedures are based on analytical procedures developed by Stein *et al.* (1993) for a planar jet at an overfall and extended by Stein and Nett (1997). Stein and Nett (1997) validated this approach in the laboratory using six different soil types.

Stein and Nett (1997) showed that as the scour hole increases with time the applied shear stress decreases, owing to increasing dissipation of jet energy within the plunge pool. Detachment rate is initially high and asymptotically approaches zero as shear stress approaches the critical shear stress of the bed material. The depth of scour at the point where the hydraulic shear is equivalent to the critical shear stress is called the equilibrium depth,  $H_e$  (Figure 2). The  $\tau_c$  for a circular submerged jet is determined by (Hanson and Cook, 1997)

$$\tau_c = \tau_0 \left( \frac{H_p}{H_e} \right)^2 \quad (2)$$

where  $H_p$  is the potential core length from the origin of the jet,  $H_e$  is the distance from the jet nozzle to the equilibrium depth of scour, and  $\tau_0$  is the maximum applied bed shear stress within the potential core. The difficulty in determining equilibrium depth is that the length of time required to reach equilibrium can be large. Blaisdell *et al.* (1981) observed during studies on pipe outlets that scour in cohesionless sands continued

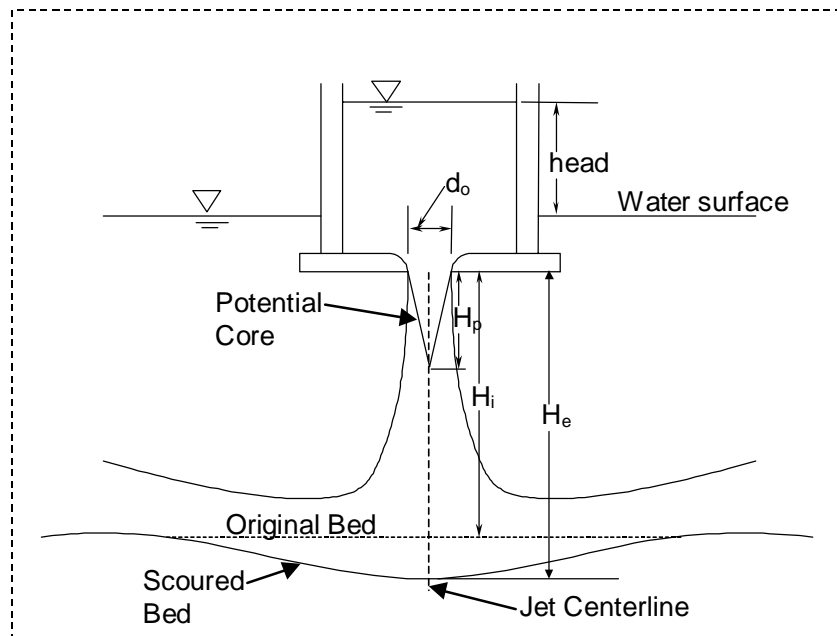


Figure 2. Schematic of jet scour parameters

to progress even after 14 months. They developed a hyperbolic function to compute the equilibrium scour depth. This method assumes that the relationship between scour and time follows a logarithmic–hyperbolic function

$$x = [(f - f_0)^2 - A^2]^{1/2} \quad (3)$$

$$x = \log \left( \frac{U_0 t}{d_0} \right) \quad (4)$$

$$f = \log \left( \frac{H}{d_0} \right) - \log \left( \frac{U_0 t}{d_0} \right) \quad (5)$$

where  $A$  is the value for the semi-transverse and semi-conjugate axis of the hyperbola,  $f_0$  is the asymptotic value of the hyperbola ( $f_0 = \log[H_e/d_0]$ ),  $U_0$  is the velocity of the jet at the origin,  $H$  is the distance from the jet nozzle to the maximum depth of scour at time  $t$ , and  $d_0$  is the diameter of the jet nozzle. As  $x$  and  $f$  are known from Equations (4) and (5), an iterative process is conducted in which the standard error is minimized based on the best-fit values of  $f_0$  and  $A$ . The value for the equilibrium depth  $H_e$  is then determined from the antilog of  $f_0$ .

The potential core length  $H_p$  and the maximum applied shear stress within the potential core  $\tau_0$  is dependent on the diffusion properties of the jet. The potential core length is defined as the distance the centreline velocity of the jet remains equal to the velocity at the jet origin,  $U_0$ . This length is defined as  $H_p = C_d d$ , where  $C_d$  is an orifice discharge coefficient with a typical value of 6.2 (Albertson *et al.*, 1950). The basic equation for modelling the erosion of a soil material beneath an impinging circular jet with an initial nozzle height  $H$  greater than the potential core length is (Hanson and Cook, 1997)

$$\frac{dH}{dt} = K_d \left[ \tau_0 \left( \frac{H_p}{H} \right)^2 - \tau_c \right] \quad (6)$$

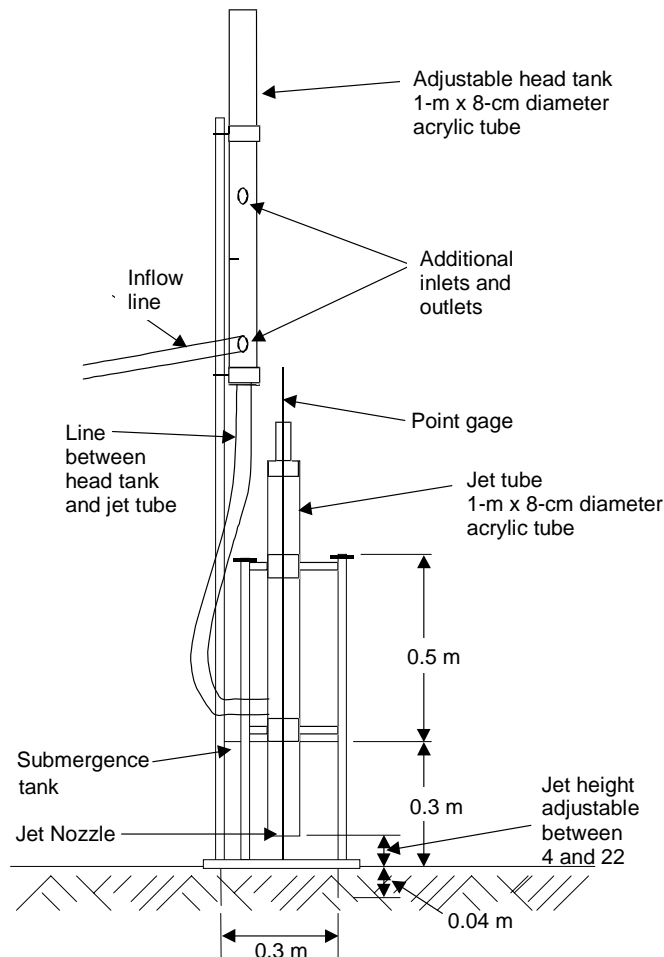
where  $dH/dt$  is the rate of scour. The maximum applied shear stress within the potential core is defined as  $\tau_0 = C_f \rho U_0^2$  where  $C_f$  is the bed coefficient of friction, and  $\rho$  is the density of water. This relationship is similar to the excess stress equation defined by Equation (1). As scour occurs beneath an impinging jet the stress at the boundary and the rate of scour change. Therefore, an integrated dimensionless form of this equation (Hanson and Cook, 1997) is used to analyse jet-test results. The equation for measured time  $t_m$  is expressed as

$$t_m = T_r \left[ 0.5 \ln \left( \frac{1 + H^*}{1 - H^*} \right) - H^* - 0.5 \ln \left( \frac{1 + H_i^*}{1 - H_i^*} \right) + H_i^* \right] \quad (7)$$

where  $t_m$  is the measured time,  $T_r = H_e/(k_d \tau_c)$ , dimensionless time  $T^* = t/T_r$ ,  $H^* = H/H_e$ , and  $H_i^* = H_i/H_p$ . The excess stress parameter  $\tau_c$  can be predetermined by fitting the scour data to the logarithmic–hyperbolic method described in Equations (3)–(5). The  $k_d$  is then determined by curve-fitting measured values of  $H$  versus  $t$  for Equation (7) and minimizing the error of the measured time  $t_m$  versus the predicted time.

#### APPARATUS AND METHODOLOGICAL APPROACH FOR *IN SITU* JET TESTING

The *in situ* jet-test apparatus consists of a pump, adjustable head tank, jet submergence tank, jet nozzle, delivery tube and point gauge (Figure 3). Water is pumped directly from the stream into an adjustable head tank. The adjustable head tank allows the user to set a desired jet velocity. The jet velocity at the nozzle origin  $U_0$ , jet height  $H_i$ , and jet diameter  $d_0$ , control the initial stress at the bed. The stress range that can be applied to the streambed using this instrument is from 4 to 1500 Pa. A head tank is designed to supply the lower stress settings from 4 to 200 Pa. Larger stresses require a direct connection from the jet tube to the

Figure 3. Schematic of *in situ* jet apparatus

pump. The jet is formed by a rounded 6.4-mm-diameter nozzle. The nozzle is submerged within a tank that is driven into the streambed. The initial height of the nozzle above the streambed can be adjusted easily prior to initiating a test. The initial height of the nozzle should be greater than the jet core length  $H_p$  (greater than six diameters). Changes in maximum bed scour are measured using a point gauge. The point gauge is aligned with the jet nozzle so that the point gauge can pass through the nozzle to the bed to read scour depth. The point-gauge diameter is nominally equivalent to the nozzle diameter so that when the point gauge rod passes through the nozzle opening, flow is effectively shut off. Maximum scour measurements are taken at 10-min intervals over a period of 120 min. It is important to note that soft streambeds require special attention in measuring the depth of scour. The user must assure that the rod is not pushed down into the bed. This is accomplished by feeling when the rod just touches the bed.

Initiation of a jet test requires placement of the submergence tank by driving it 0.04 m into the bed. Once the submergence tank is set in the bed, the jet tube and adjustable head tank are attached. The jet tube is attached to a hanger that orientates the tube in the centre of the submergence tank. The head tank is attached to a mast that allows the user to move it up or down. The head tank controls the pressure delivered to the jet nozzle and, in turn, the jet velocity. The operator, using markings on the side of the jet tube, estimates the initial height of the jet nozzle. Once the jet nozzle is set, the initial jet height ( $H_i$ ) is measured more precisely

using the point gauge. Following a determination of the bed elevation relative to the jet nozzle, the head is set by holding a plate downstream of the jet nozzle to divert the impinging jet. Once the head is set testing can begin by removing the plate and allowing the jet to impinge on the bed.

The first calculation is the equilibrium scour depth. A hyperbolic function developed by Blaisdell *et al.* (1981) is used to compute the equilibrium scour depth based on Equation (3) (Figure 4). The  $\tau_c$  is, therefore, estimated from the equilibrium depth (Equation 2). Once the equilibrium depth and  $\tau_c$  are determined,  $k_d$  is determined from the measurements of scour depth and time (Figure 5). The best value of  $k_d$  is determined based on the minimization of the standard error for the predicted time versus the measured time of scour obtained from Equation (7).

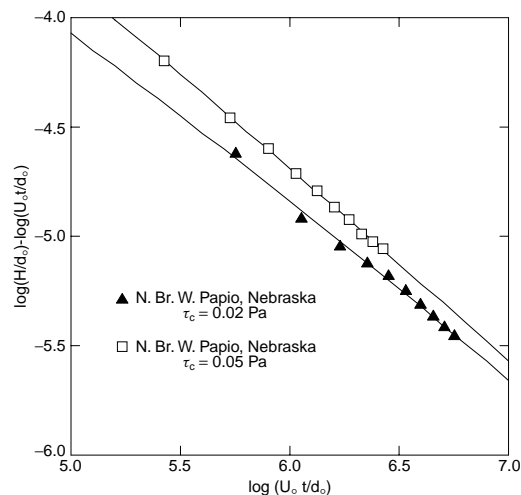


Figure 4. Logarithmic hyperbolic curve fit of jet-test results to determine critical shear stress

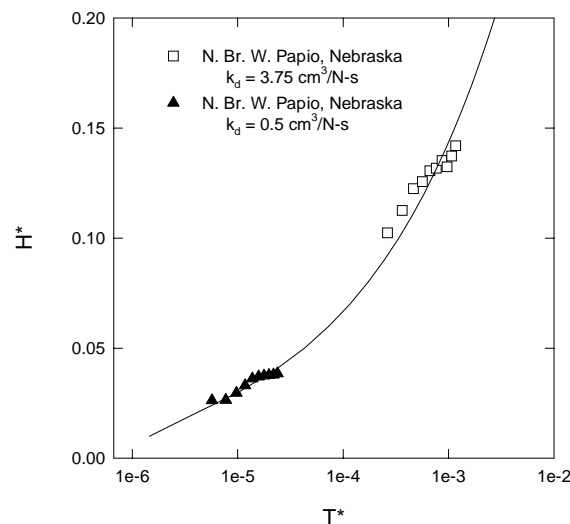


Figure 5. Scour function of dimensionless time and depth to determine  $k_d$

## IN-SITU STREAMBED TESTS

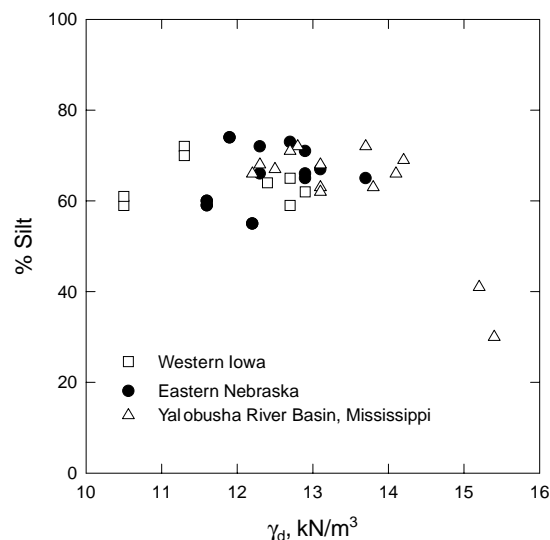
Results from 83 submerged jet tests conducted in cohesive streambeds in several streams in south-eastern Nebraska, south-western Iowa, and the Yalobusha River Basin in north-central Mississippi are summarized in this paper (Figure 1). These streambeds are located in the highly erodible loess area of the midwestern USA. Analysis of soil samples taken from these beds indicate that they are typically silt-bedded channels with 50 to 80% silt-sized materials with a dry unit weight varying roughly from 11 to 15 kN/m<sup>3</sup> (Figure 6).

Observations of the relative frequency of  $\tau_c$  (Figure 7a) and  $k_d$  (Figure 7b) for the tests conducted in each area give another view of their respective erosion resistance. The  $\tau_c$  for 70% of the tested materials in western Iowa were in the lowest class, and 100% in the lowest three classes; whereas nearly 50% of the tests conducted in the Yalobusha River Basin, Mississippi were in the upper class. For  $\tau_c$  values the lower the class the lower the resistance. The  $k_d$  test values were broken into four classes, with western Iowa results having close to 80% in the upper two classes and the Yalobusha River Basin having close to 70% in the lower two classes. For  $k_d$ , the lower the class the greater the resistance to erosion. These results indicate that cohesive streambed materials in western Iowa are the least resistant to erosion; whereas those in the Yalobusha River Basin are generally the most resistant to erosion.

Results indicate that there is a wide variation in the erosion resistance of the streambeds, spanning six orders of magnitude for  $\tau_c$  and four orders of magnitude for  $k_d$  (Figure 8; Table I). The most erodible bed materials that were tested were in south-eastern Nebraska, with  $\tau_c$  close to 0.0 and  $k_d$  as high as 3.75 cm<sup>3</sup>/N-s. These beds consisted of loess-derived alluvium originating from failed bank materials and deposited silts. These beds scoured rapidly even under low stresses from the jet. The most resistant bed materials were observed in the Yalobusha River Basin, Mississippi. The highest measured  $\tau_c$  was 400 Pa and the lowest  $k_d$  was 0.001 cm<sup>3</sup>/N-s.

An inverse relationship between  $\tau_c$  and  $k_d$  was observed, where soils exhibiting a low  $\tau_c$  have a high  $k_d$  and soils having a high  $\tau_c$  tend to have a low  $k_d$ . Some of the same trends were also observed by Arulanandan *et al.* (1980) during laboratory flume testing of soil samples from cohesive streambed materials obtained across the USA. The measure of material resistance to hydraulic stresses is a function of both  $\tau_c$  and  $k_d$ . Based on our observations,  $k_d$  can be estimated as a function of  $\tau_c$  ( $r^2 = 0.64$ ):

$$k_d = 0.2\tau_c^{-0.5} \quad (8)$$



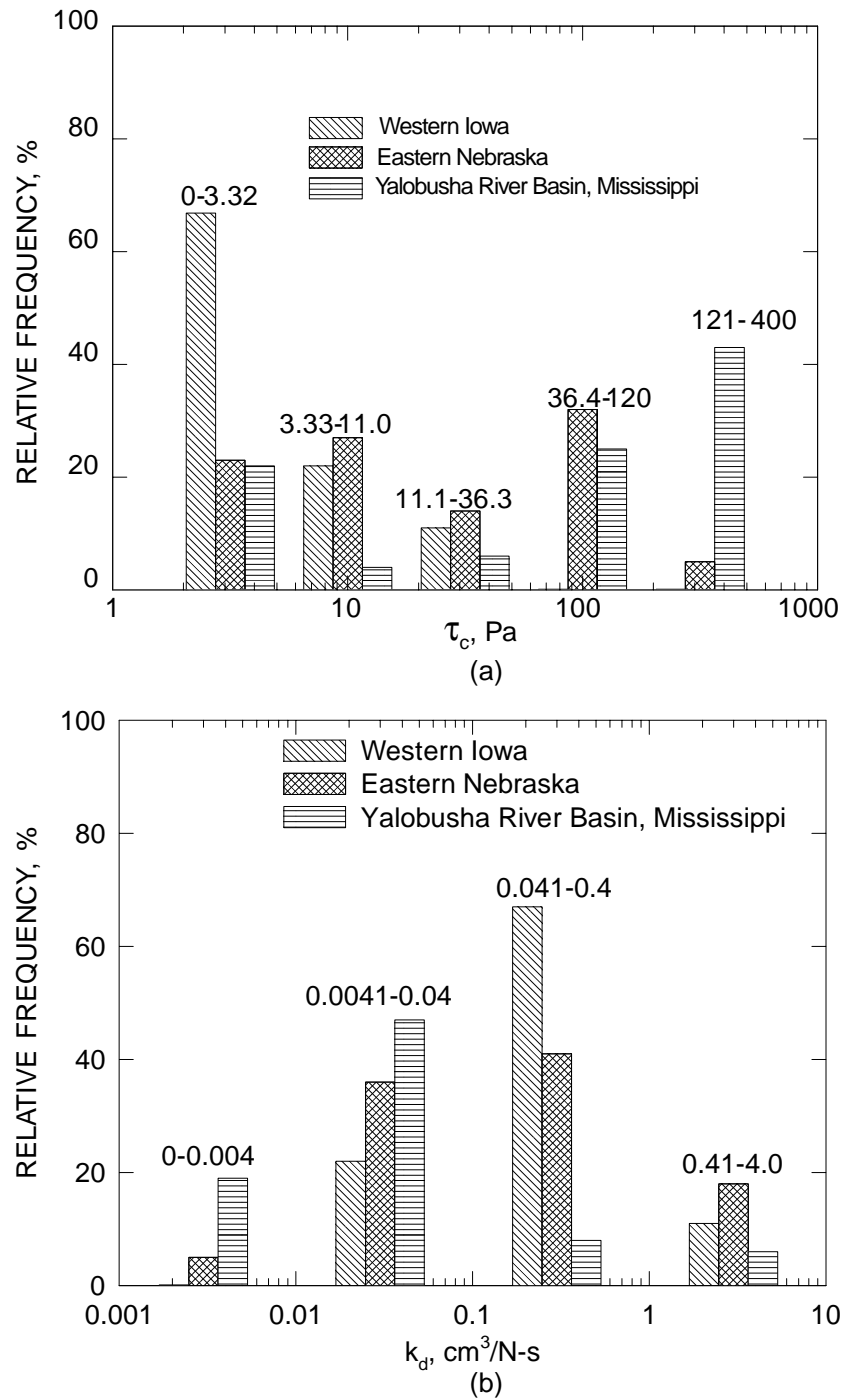
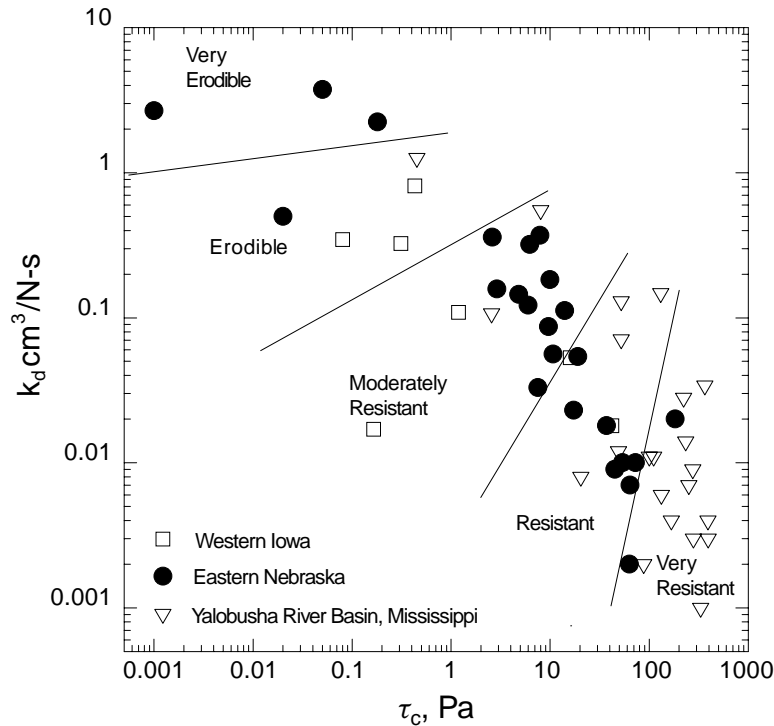


Figure 7. Relative frequency distribution of critical shear stresses (a) and erodibility coefficient (b) for jet-test results of streambeds

To relate these values to the relative potential for flows to erode cohesive beds (by Equation 1) and to compare cohesive resistance to the resistance of a non-cohesive particle (equivalent diameter), an average

Figure 8.  $\tau_c$  versus  $k_d$  from cohesive streambed tests

boundary-shear stress is calculated

$$\tau_0 = \gamma y S \quad (9)$$

where  $\gamma$  is the unit weight of water ( $\text{N/m}^3$ ),  $y$  is flow depth (m) and  $S$  is water-surface slope (m/m). The Shields criteria is invoked to then calculate the equivalent particle diameter for the measured critical shear stresses

$$\tau^* = \tau_0 / (\gamma_s - \gamma) d \quad (10)$$

where  $\tau^*$  is the critical dimensionless shear stress,  $\gamma_s$  is the unit weight of sediment in  $\text{N/m}^3$  and  $d$  is a representative particle diameter (m).

Data from the Yalobusha River Basin are used as an example because of the broad range of  $k_d$  values and the large number of jet tests conducted in the watershed. Using a bed slope of 0.001 m/m and a flow depth of 8 m (approximately bankfull in a reach of migrating knickpoints in the Yalobusha River; Simon, 1998), boundary shear stress is calculated to be about 78 Pa by Equation (9). This shear stress is generally not sufficient to erode many of the *in situ* clay beds, a steeper gradient and/or depth being required. Shear stresses generated for a range of slopes (0.001–0.004) and flow depths (4, 6 and 8 m) are shown in Table II. Using the mean, measured critical shear stress for this river system of 130 Pa, substituting this value into Equation (10), and assuming  $\tau^* = 0.03$  and  $(\gamma_s - \gamma) = 1650 \text{ kg/m}^3 \times 9.81 \text{ m/s}^2$ , results in an equivalent particle diameter  $d$  of about 27 cm. Erosion of the clay beds is, therefore, equivalent to entraining non-cohesive clasts with diameters of about 27 cm. By using other conventional values of  $\tau^*$ , such as 0.047 and 0.06, equivalent particle diameters become 17 and 14 cm, respectively. Calculations of equivalent particle diameters for all tests are shown in Table III.

Mean values, however, probably do not provide an accurate picture of streambed  $k_d$  characteristics in the Yalobusha River Basin in that the distribution of critical shear stresses is highly skewed to low and high

Table I. Critical shear stress ( $\tau_c$ ) and erodibility coefficient ( $k$ ) values for tests in the Yalobusha River System, Mississippi

Site	$\tau_c$ (Pa)	$k_d$ (cm <sup>3</sup> /N-s)	Site	$\tau_c$ (Pa)	$k_d$ (cm <sup>3</sup> /N-s)
Bear Creek B3	260	0.006	Johnson Creek—upper unit	0.39	0.164
Bear Creek B3C	1.99	0.096	Johnson Creek—upper unit	1.31	0.120
Bear Creek B3C	5.48	0.042	Johnson Dry 1	0.378	0.095
Big Creek 5C (d/s)	49	0.012	Little Topashaw LT1	63.6	0.012
Big Creek 5C (u/s)	133	0.006	Little Topashaw LT1	44.9	0.019
Big Creek Big6	8	0.551	Mud Dry 1	93.5	0.064
Big Creek Big6	0.45	1.264	Mud Dry 2	180.8	0.015
Big Creek Big6	2.57	0.107	Mud Wet 1	84.5	0.006
Big Creek Big6	223	0.028	Mud Wet 2	20.5	0.073
Big Creek Big6	20.4	0.008	Porters Creek, Tenn.	58	0.016
Buck Creek Bu1	111	0.011	Topashaw Creek T6	88	0.002
Buck Creek Bu1	252	0.007	Topashaw Creek T6	331	0.001
Buck Creek Bu1	333	0.004	Topashaw Creek T6	393	0.003
Buck Creek Bu1	275	0.009	Topashaw T2-C1	219.7	0.004
Buck Creek Bu1	131	0.148	Topashaw T4 Dry	264.9	0.029
Buck Creek Bu2	13.4	0.028	Topashaw T4 Wet	183.1	0.005
Buck Creek Bu2	3.26	0.050	Topashaw T7	281	0.002
Bull Dry Test 1	215.30	0.003	Topashaw T7	400	0.007
Bull Wet Test 1	133.3	0.006	Topashaw Trib 1 TT1-1 (d/s; weathered)	52	0.130
Bull Wet Test 2	376.4	0.007	Topashaw Trib 1 TT1-1 (d/s; weathered)	52	0.071
Cane Creek C-0	73	0.009	Topashaw Trib 1 TT1-1 (u/s)	392	0.004
Cane Creek C-0	95	0.011	Topashaw Trib 1 TT1-1 (u/s)	167	0.004
Cane Creek C4	364	0.034	Yalobusha D/S Pyland	15.1	0.150
Cane Creek C4	234	0.014	Yalobusha D/S Pyland	2.48	0.050
Johnson Creek—lower unit	1.55	0.016	Yalobusha @ Johnson Wet 1	0.749	0.118
Johnson Creek—lower unit	69	0.006	Yalobusha @ Johnson Wet 2	0.467	0.088
Average	135.47	0.07			
Median	93.5	0.012			
Maximum	400.0	1.3			
Minimum	0.38	0.00			
Standard deviation	129.3	0.2			

Table II. Range of shear stresses ( $\tau_c$ ) for varying water-surface slopes and flow depths. *Italic typeface denotes data used as represented maxima for zone of migrating knick-points*

Flow depth (m)	Water-surface slope (m/m)	$\tau$ (Pa)
8	<i>0.001</i>	78
8	<i>0.002</i>	157
8	<i>0.003</i>	235
8	<i>0.004</i>	314
6	0.001	59
6	0.002	118
6	0.003	177
6	0.004	235
4	0.001	39
4	0.002	78
4	0.003	118
4	0.004	157

Table III. Range of equivalent diameters for tested streambeds using  $\tau^* = 0.03, 0.047$  and  $0.06$ 

Site	Equivalent diameter, $\tau^* = 0.03$ (cm)	Equivalent diameter, $\tau^* = 0.047$ (cm)	Equivalent diameter, $\tau^* = 0.06$ (cm)
Bear Creek B3	53.54	34.18	26.77
Bear Creek B3C	0.41	0.26	0.20
Bear Creek B3C	1.13	0.72	0.56
Big Creek 5C (d/s)	10.09	6.44	5.05
Big Creek 5C (u/s)	27.39	17.48	13.69
Big Creek Big6	1.65	1.05	0.82
Big Creek Big6	0.09	0.06	0.05
Big Creek Big6	0.53	0.34	0.26
Big Creek Big6	45.92	29.31	22.96
Big Creek Big6	4.20	2.68	2.10
Buck Creek Bu1	22.86	14.59	11.43
Buck Creek Bu1	51.90	33.12	25.95
Buck Creek Bu1	68.58	43.77	34.29
Buck Creek Bu1	56.63	36.15	28.32
Buck Creek Bu1	26.98	17.22	13.49
Buck Creek Bu2	2.76	1.76	1.38
Buck Creek Bu2	0.67	0.43	0.34
Bull Dry Test 1	44.33	28.30	22.17
Bull Wet Test 1	27.45	17.52	13.73
Bull Wet Test 2	77.51	49.48	38.26
Cane Creek C-0	15.03	9.60	7.52
Cane Creek C-0	19.56	12.49	9.78
Cane Creek C4	74.96	47.85	37.48
Cane Creek C4	48.19	30.76	24.09
Johnson Creek—lower unit	0.32	0.20	0.16
Johnson Creek—lower unit	14.21	9.07	7.10
Johnson Creek—upper unit	0.08	0.05	0.04
Johnson Creek—upper unit	0.27	0.17	0.13
Johnson Dry 1	0.08	0.05	0.04
Little Topashaw LT1	13.10	8.36	6.5
Little Topashaw LT1	9.25	5.90	4.62
Mud Dry 1	19.25	12.29	9.63
Mud Dry 2	37.23	23.77	18.62
Mud Wet 1	17.40	11.11	8.70
Mud Wet 2	4.22	2.69	2.11
Porters Creek, Tenn.	11.94	7.62	5.97
Topashaw Creek T6	11.12	11.57	9.06
Topashaw Creek T6	68.16	43.51	34.08
Topashaw Creek T6	80.93	51.66	40.47
Topashaw T2-C1	45.24	28.88	22.62
Topashaw T4 Dry	54.55	34.82	27.28
Topashaw T4 Wet	37.71	24.07	18.85
Topashaw T7	57.87	36.94	28.93
Topashaw T7	82.37	52.58	41.19
Topashaw Trib 1 TT1-1 (d/s; weathered)	10.71	6.84	5.35
Topashaw Trib 1 TT1-1 (d/s; weathered)	10.71	6.84	5.35
Topashaw Trib 1 TT1-1 (u/s)	80.73	51.53	40.36
Topashaw Trib 1 TT1-1 (u/s)	34.39	21.95	17.20
Yalobusha D/S Pyland	3.11	1.98	1.55
Yalobusha D/S Pyland	0.51	0.33	0.26
Yalobusha @ Johnson Wet 1	0.15	0.10	0.08

(continued overleaf)

Table III. (continued)

Site	Equivalent diameter, $\tau^* = 0.03$ (cm)	Equivalent diameter, $\tau^* = 0.047$ (cm)	Equivalent diameter, $\tau^* = 0.06$ (cm)
Yalobusha @ Johnson Wet 2	0.10	0.06	0.05
Average	26.83	17.12	13.41
Median	17.76	11.34	8.88
Maximum	82.37	52.58	41.19
Minimum	0.08	0.05	0.04

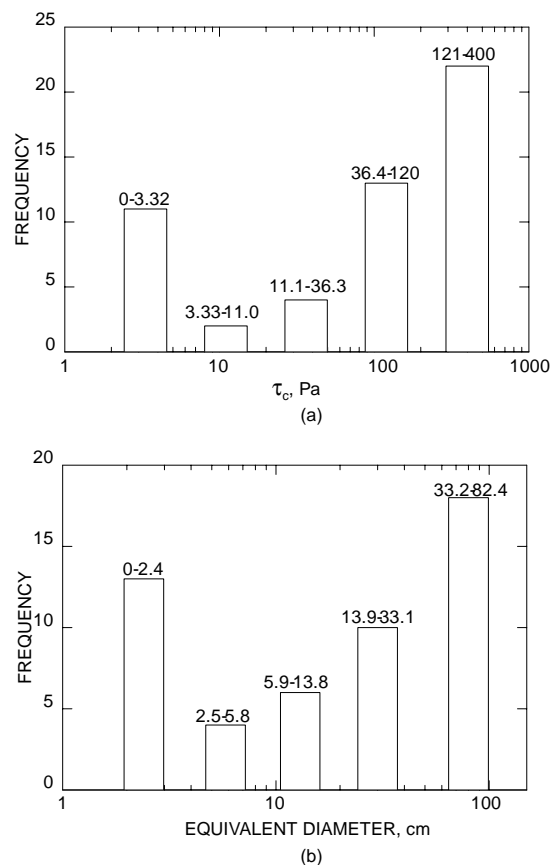


Figure 9. Frequency distribution of critical shear stresses (a) and equivalent particle diameters (b) for jet tests in the Yalobusha River Basin, Mississippi

values, representing at least two different material types (Figure 9a). As one might expect, a similar skewed distribution is shown for equivalent particle diameters in Figure 9b. The upper class of Figure 9 represents the Porters Creek Clay Formation while the lowest class probably represents the overlying Naheola Formation, both belonging to the Midway Group of Paleocene age (Parks, 1961). Orders of magnitude variation of  $\tau_c$  within each material type is believed to be a function of varying degrees of subaerial exposure, weathering and the amount of cracking along bedding planes and other planes of weakness.

To account for the diversity of the two primary materials making up the streambeds, the median value of  $\tau_c$  for each of the two extreme classes (1.31 and 256 Pa) are used with the original assumptions of an

Table IV. Equivalent diameters for Naheola and Porters Creek Clay Formations using  $\tau^* = 0.03, 0.047$  and  $0.06$ 

Formation	Equivalent diameter, $\tau^* = 0.03$ (cm)	Equivalent diameter, $\tau^* = 0.047$ (cm)	Equivalent diameter, $\tau^* = 0.06$ (cm)
Naheola	0.27	0.17	0.13
Porters	52.72	33.65	26.36

8-m flow depth and a slope of 0.001 m/m. Again using  $\tau^*$  values of 0.03, 0.047 and 0.06 (Vanoni, 1975) results in equivalent diameters ranging from 26 to 53 cm and from 0.13 to 0.27 cm for the Porters Creek Clay and Naheola Formations, respectively (Table IV). Clearly, most flows will be competent to erode streambeds composed of the Naheola Formation ( $\tau_c = 1.31$  Pa). In contrast, only the deepest (8 m) flows with profiles steeper than 0.003 m/m generate average boundary-shear stresses great enough to erode streambeds composed of the Porters Creek Clay Formation (Table II).

Although the 'representative' average boundary-shear stress of 78 Pa was insufficient to erode an 'average' cohesive streambed in the Yalobusha River Basin, local shear stresses as great as 225 Pa have been calculated from flow-depth and water-surface slope data in the vicinity of knickpoints. Based on  $\tau_c$  data obtained from jet testing, shear stresses of this magnitude are apparently capable of eroding some of the knickpoint zones, particularly those cut into the Naheola Formation. Rates of erosion ( $\varepsilon$ ) in centimetres per second were calculated by Equation (1) for all study sites in the Yalobusha River Basin by assuming a range of steady-flow conditions with boundary-shear stresses of 50, 100, 150, 200, 250 and 300 Pa. Strictly adhering to Equation (1) produces negative values of  $\varepsilon$  for non-erodible conditions. Because these have no actual physical meaning, they have been converted to 0.0 in Table V. By again using the median values of  $\tau_c$  for the two dominant formations and by including the median values of  $k_d$  'representative' erosion rates (from Equation 1) can be obtained under the given shear stress conditions. As indicated previously, streambeds composed of the Porters Creek Clay Formation are shown to be non-erodible until flows of about 300 Pa are encountered. At this shear stress, these beds can erode via particle-by-particle detachment, but only slowly, at a rate of  $2.6 \times 10^{-5}$  cm/s (Table V). Streambeds composed of the Naheola Formation are readily eroded over the entire range of shear stresses at rates of  $4.7 \times 10^{-4}$  to  $2.9 \times 10^{-3}$  cm/s (Table V).

With maximum  $\tau_c$  values reaching almost 400 Pa, erosion of these more resistant materials occurs by forces and mechanisms other than by the shear of flowing water. These processes include, but are probably not limited to, upward-directed seepage forces and stress deformation through negative effective stresses (Simon *et al.*, in press).

## SUMMARY

Streambeds, predominantly in three areas, western Iowa, eastern Nebraska, and the Yalobusha River Basin, Mississippi, were tested using an *in situ* jet-testing apparatus to determine the erosion resistance of the cohesive materials. The analysis of the jet tests is based on the theoretical development of jet diffusion characteristics of a submerged circular jet. The analysis of the data sets focuses on the changes in scour with time for the cohesive bed material. The excess stress parameters  $\tau_c$  and  $k_d$  determined from the jet test results are used to assess erosion resistance of the cohesive bed materials.

Critical stress was observed to vary over a range of six orders of magnitude and  $k_d$  over a range of four orders of magnitude. The streambeds in the Yalobusha River Basin were observed to have the most resistant materials, with  $\tau_c$  as high as 400 Pa. The weakest materials tested were in eastern Nebraska, with  $\tau_c$  less than 0.001 Pa. These materials were apparently derived from bank failures. There were also very resistant beds observed in eastern Nebraska. The materials tested in western Iowa ranged from resistant to erodible, with no materials observed as resistant as south-eastern Nebraska or the Yalobusha River Basin.

Table V. Rates of erosion for all test locations and for Porters Creek and Naheola Formations assuming  $\tau = 50, 100, 150, 200, 250$  and  $300$  Pa. Note  $\varepsilon_{100}$  = erosion rate for an applied shear stress of  $50$  Pa

Site	$\varepsilon_{50}$ (cm/s)	$\varepsilon_{100}$ (cm/s)	$\varepsilon_{150}$ (cm/s)	$\varepsilon_{200}$ (cm/s)	$\varepsilon_{250}$ (cm/s)	$\varepsilon_{300}$ (cm/s)
Bear Creek B3	0.00	0.00	0.00	0.00	0.00	240E-05
Bear Creek B3C	4.61E-04	9.41E-04	1.42E-03	1.90E-03	2.38E-03	2.86E-03
Bear Creek B3C	1.87E-04	3.97E-04	6.07E-04	8.17E-04	1.03E-03	1.24E-03
Big Creek 5C (d/s)	1.00E-06	6.10E-05	1.21E-04	1.81E-04	2.41E-04	3.01E-04
Big Creek 5C (u/s)	0.00	0.00	1.00E-05	4.00E-05	7.00E-05	1.00E-04
Big Creek Big6	2.31E-03	5.07E-03	7.82E-03	1.06E-02	1.33E-02	1.61E-02
Big Creek Big6	6.26E-03	1.26E-02	1.89E-02	2.52E-02	3.15E-02	3.79E-02
Big Creek Big6	5.08E-04	1.04E-03	1.58E-03	2.11E-03	2.65E-03	3.18E-03
Big Creek Big6	0.00	0.00	0.00	0.00	7.60E-05	2.16E-04
Big Creek Big6	2.40E-05	6.40E-05	1.04E-04	1.44E-04	1.84E-04	2.24E-04
Buck Creek Bu1	0.00	0.00	4.30E-05	9.80E-05	1.53E-04	2.08E-04
Buck Creek Bu1	0.00	0.00	0.00	0.00	0.00	3.40E-05
Buck Creek Bu1	0.00	0.00	0.00	0.00	0.00	0.00
Buck Creek Bu1	0.00	0.00	0.00	0.00	0.00	2.30E-05
Buck Creek Bu1	0.00	0.00	2.81E-04	1.02E-03	1.76E-03	2.50E-03
Buck Creek Bu2	1.02E-04	2.42E-04	3.82E-04	5.22E-04	6.62E-04	8.02E-04
Buck Creek Bu2	2.43E-04	4.84E-04	7.43E-04	9.84E-04	1.23E-03	1.48E-03
Bull Dry Test 1	0.00	0.00	0.00	0.00	1.00E-05	2.50E-05
Bull Wet Test 1	0.00	0.00	1.00E-05	4.00E-05	7.00E-05	1.00E-04
Bull Wet Test 2	0.00	0.00	0.00	0.00	0.00	0.00
Cane Creek C-0	0.00	2.40E-05	6.90E-05	1.14E-04	1.59E-04	2.04E-04
Cane Creek C-0	0.00	6.00E-06	6.10E-05	1.16E-04	1.71E-04	2.26E-04
Cane Creek C4	0.00	0.00	0.00	0.00	0.00	0.00
Cane Creek C4	0.00	0.00	0.00	0.00	2.20E-05	9.20E-05
Johnson Creek—lower unit	7.80E-05	1.58E-04	2.38E-04	3.18E-04	3.98E-04	4.78E-04
Johnson Creek—lower unit	0.00	1.90E-05	4.90E-05	7.90E-05	1.09E-04	1.39E-04
Johnson Creek—upper unit	8.14E-04	1.63E-03	2.45E-03	3.27E-03	4.09E-03	4.91E-03
Johnson Creek—upper unit	5.84E-04	1.18E-03	1.78E-03	2.83E-03	2.98E-03	3.58E-03
Johnson Dry 1	4.71E-04	9.46E-04	1.42E-03	1.90E-03	2.37E-03	2.85E-03
Little Topashaw LT1	0.00	4.40E-05	1.04E-04	1.64E-04	2.24E-04	2.84E-04
Little Topashaw LT1	1.00E-05	1.05E-04	2.00E-04	2.95E-04	3.90E-04	4.85E-04
Mud Dry 1	0.00	4.20E-05	3.62E-04	6.82E-04	1.00E-03	1.32E-03
Mud Dry 2	0.00	0.00	0.00	2.90E-05	1.04E-04	1.79E-04
Mud Wet 1	0.00	9.00E-06	3.90E-05	6.90E-05	9.90E-05	1.29E-04
Mud Wet 2	2.15E-04	5.80E-04	9.45E-04	1.31E-03	1.68E-03	2.04E-03
Porters Creek, Tenn.	0.00	6.70E-05	1.47E-04	2.27E-04	3.07E-04	3.87E-04
Topashaw Creek T6	0.00	2.00E-06	1.20E-05	2.20E-05	3.20E-05	4.20E-05
Topashaw Creek T6	0.00	0.00	0.00	0.00	0.00	0.00
Topashaw Creek T6	0.00	0.00	0.00	0.00	0.00	0.00
Topashaw T2-C1	0.00	0.00	0.00	0.00	1.20E-05	3.20E-05
Topashaw T4 Dry	0.00	0.00	0.00	0.00	0.00	1.02E-04
Topashaw T4 Wet	0.00	0.00	0.00	8.00E-06	3.30E-05	5.80E-05
Topashaw T7	0.00	0.00	0.00	0.00	0.00	4.00E-06
Topashaw T7	0.00	0.00	0.00	0.00	0.00	0.00
Topashaw Trib 1 TT1-1 (d/s; weathered)	0.00	6.24E-04	1.27E-03	1.92E-03	2.57E-03	3.22E-03
Topashaw Trib 1 TT1-1 (d/s; weathered)	0.00	3.41E-04	6.96E-04	1.05E-03	1.41E-03	1.76E-03
Topashaw Trib 1 TT1-1 (u/s)	0.00	0.00	0.00	0.00	0.00	0.00
Topashaw Trib 1 TT1-1 (u/s)	0.00	0.00	0.00	1.30E-05	3.30E-05	5.30E-05
Yalobusha D/S Pyland	5.24E-04	1.27E-03	2.02E-03	2.77E-03	3.52E-03	4.27E-03
Yalobusha D/S Pyland	2.38E-04	4.88E-04	7.38E-04	9.88E-04	1.24E-03	1.49E-03
Yalobusha @ Johnson Wet 1	5.81E-04	1.17E-03	1.76E-03	2.35E-03	2.94E-03	3.53E-03

(continued on next page)

Table V. (continued)

Site	$\varepsilon_{50}$ (cm/s)	$\varepsilon_{100}$ (cm/s)	$\varepsilon_{150}$ (cm/s)	$\varepsilon_{200}$ (cm/s)	$\varepsilon_{250}$ (cm/s)	$\varepsilon_{300}$ (cm/s)
Yalobusha @ Johnson Wet 2	4.36E-04	8.76E-04	1.32E-03	1.76E-03	2.20E-03	2.64E-03
Porters Creek Clay Formation	0.00	0.00	0.00	0.00	0.00	2.60E-05
Naheola Formation	4.67E-04	9.47E-04	1.43E-03	1.90E-03	2.39E-03	2.87E-03
Average	2.70E-04	5.86E-04	9.18E-04	1.26E-03	1.61E-03	1.96E-03
Median	0.00	1.40E-05	6.50E-05	1.15E-04	1.65E-04	2.20E-04
Maximum	6.26E-03	1.26E-02	1.89E-02	2.52E-02	3.15E-02	3.79E-02
Minimum	0.00	0.00	0.00	0.00	0.00	0.00
Standard deviation	9.23E-04	1.87E-03	2.82E-03	3.76E-03	4.71E-03	5.65E-03

Therefore, this may indicate that if the systems have the same flow-energy levels, the western Iowa streambeds may experience more severe degradation problems in the future. This will require a more detailed mapping of the location of materials and of flow-energy levels within the systems before this can be considered conclusive.

The other observation that was made with the jet tests is that these stream systems may consist of several materials exposed in the streambeds with various levels of erosion resistance. The Yalobusha River is a good example where the distribution of critical stresses are highly skewed to low and high values representing at least two different materials, the Porters Creek Clay and Naheola Formations. Observed orders of magnitude variation of  $\tau_c$  within each material type is a function of varying degrees of subaerial exposure, weathering and the amount of cracking along bedding planes and other planes of weakness. The number of tests that have been conducted and are planned for the incised Yalobusha River System should allow for detailed mapping of these materials and help locate areas of particular concern.

## REFERENCES

- Albertson ML, Dai YB, Jensen RA, Rouse H. 1950. Diffusion of submerged jets. *American Society of Civil Engineers* **2509**: 639–664.
- ASTM. 1995. *Annual Book of ASTM Standards: Section 4, Construction*, vol. 04.09. American Society for Testing and Materials. West Conshohocken, PA.
- Arulanandan K, Gillogley E, Tully R. 1980. *Development of a Quantitative Method to Predict Critical Shear Stress and Rate of Erosion of Natural Undisturbed Cohesive Soils*. Waterway Experiment Station Technical Report GL-80-5, University of California at Davis: Davis, CA.
- Blaisdell FW, Clayton LA, Hebaus GG. 1981. Ultimate dimension of local scour. *Journal of Hydraulics Division, American Society of Civil Engineers* **107**(HY3): 327–337.
- Dunn IS. 1959. Tractive resistance of cohesive channels. *Proceedings Journal of Soil Mechanics and Foundation Division, American Society of Civil Engineers* **85**(SM3): 1–24.
- Grissinger EH. 1982. Bank erosion of cohesive materials. In *Gravel-bed Rivers*, Hey RD, Bathurst JC, Thorne CR (eds). Wiley: Chichester; 273–287.
- Hanson GJ. 1990. Surface erodibility of earthen channels at high stresses. Part II—developing an *in situ* testing device. *Transactions of the American Society of Agricultural Engineers* **33**(1): 132–137.
- Hanson GJ. 1991. Development of a jet index to characterize erosion resistance of soils in earthen spillways. *Transactions of the American Society of Agricultural Engineers* **36**(5): 2015–2352.
- Hanson GJ, Cook KR. 1997. Development of excess shear stress parameters for circular jet testing. ASAE Paper No. 97–2227, American Society of Agricultural Engineers: St. Joseph, MI.
- Hanson GJ, Robinson KR. 1993. The influence of soil moisture and compaction on spillway erosion. *Transactions of the American Society of Agricultural Engineers* **36**(5): 1349–1352.
- Hollick M. 1976. Towards a routine test for the assessment of the critical tractive forces of cohesive soils. *Transactions of the American Society of Agricultural Engineers* **19**(6): 1076–1081.
- Lutenegger AJ. 1987. *In situ* shear strength of friable loess. In *Loess and Environment*, vol. 9, Pesci M (ed.), Catena Supplement; 27–34.
- Moore WL, Masch FD. 1962. Experiments of the scour resistance of cohesive sediments. *Journal of Geophysical Research* **67**(4): 1437–1446.
- Parks WS. 1961. Calhoun County geology and ground-water resources. *Mississippi Geological Survey Bulletin* **92**: 113.
- Simon A. 1998. *Processes and forms of the Yalobusha River System: a Detailed Geomorphic Evaluation*. National Sedimentation Laboratory Research Report No. 9, US Department of Agriculture, Agricultural Research Service: 131 pp.
- Simon A, Curini A, Hanson GJ, Collison AJ. In press. Pore pressure effects on the entrainment and erosion of cohesive streambeds and streambanks in incised channels: Seepage forces and matric suction. *Earth Surface Processes and Landforms*.

- Stein OR, Nett DD. 1997. Impinging jet calibration of excess shear sediment detachment parameters. *Transactions of the American Society of Agricultural Engineers* **40**(6): 1573–1580.
- Stein OR, Julien PY, Alonso CV. 1993. Mechanics of jet scour downstream of a headcut. *Journal of Hydraulic Research* **31**(6): 723–738.
- Vanoni VA. 1975. Sedimentation Engineering. *ASCE Manuals and Reports on Engineering Practice No. 54*. American Society of Civil Engineers: Reston, VA; 745 pp.